

Violation of C/CP Symmetry Induced by a Scalar Field Emerging from a Two-Brane Universe: A Gateway to Baryogenesis and Dark Matter

Michaël Sarrazin^{1,2,*} and Coraline Stasser²

¹*Institut UTINAM, CNRS/INSU, UMR 6213, Université Bourgogne-Franche-Comté,
16 route de Gray, F-25030 Besançon Cedex, France*

²*Laboratory of Analysis by Nuclear Reactions, Department of Physics,
University of Namur, 61 rue de Bruxelles, B-5000 Namur, Belgium*

A model of baryogenesis is introduced where our usual visible Universe is a 3-brane coevolving with a hidden 3-brane in a multidimensional bulk. The visible matter and antimatter sectors are naturally coupled with the hidden matter and antimatter sectors, breaking the C/CP invariance and leading to baryogenesis occurring after the quark-gluon era. The issue of leptogenesis is also discussed. The symmetry breaking spontaneously occurs in relation to the presence of an extra scalar field supported by the $U(1) \otimes U(1)$ gauge group, which extends the conventional electromagnetic gauge field in the two-brane universe. Scalar waves also emerge as potential dark matter candidates and a means of constraining the model.

I. INTRODUCTION

While the standard model of particle physics and the concordance model of cosmology have achieved predictive success, there are still puzzling data that require interpretation. These include for instance the observations of dark matter and dark energy [1], as well as the matter-antimatter asymmetry [2–4]. Our Universe is mainly empty space, with a mean baryonic matter density about one proton per 4 cubic meters. However, such a value is extremely large and the absence of antimatter raises significant questions. Indeed, shortly after the initial moment of the Big Bang, particles and antiparticles should have been in thermal equilibrium with the photon bath. As the Universe expanded, matter and antimatter should have almost completely annihilated once the global temperature dropped below the mass energy of each particle. Nevertheless, a large baryon-antibaryon asymmetry is observed, with the visible Universe today dominated by matter rather than antimatter [2–4]. This is the baryogenesis problem. Those unresolved issues, coupled with the quest for a unified theory of fundamental interactions, have motivated extensive theoretical work, resulting in a diverse landscape of models that challenge new experimental projects aimed at testing new physics [1, 2, 5–8]. In this context, many theoretical works suggest that our visible Universe could be a 3-dimensional physical entity (a 3-brane) embedded in a $(3 + N, 1)$ –space-time ($N \geq 1$) known as the bulk [9–15]. Hidden 3-branes may coexist alongside our own in the bulk. This leads to a rich phenomenology encompassing both particle physics and cosmology [7]. Some studies propose that hidden branes could host dark matter, or that interactions between branes could account for dark energy [16–21]. In addition, many scenarios suggest that the Big Bang was triggered by a collision between our visible brane and a hidden one [22–33]. Previous research has highlighted

that braneworld scenarios or dark matter models involving sterile particles could explain baryogenesis [34, 35].

Moreover, numerous theoretical predictions have emerged regarding hidden or dark sectors, allowing phenomena like neutron–hidden neutron transitions $n - n'$ [8, 36]. Over the past decade, this phenomenology has prompted efforts to constrain these scenarios through neutron disappearance/reappearance experiments [37–43]. Specifically, a neutron n in our visible brane can transmute into a hidden neutron n' , effectively swapping into a hidden brane [44–47], depending on a specific coupling constant g between visible and hidden sectors. The theoretical study of this brane phenomenology [44–47] has been complemented by experimental tests over the past two decades [37–41], particularly through passing-through-wall neutron experiments [38, 39], which have provided stringent bounds on the coupling constant g [40, 41].

In the present paper, assuming previous theoretical results [45–47], one shows how a two-brane universe provides a solution to the baryogenesis issue after the phase transition from quark-gluon plasma to hadron gas. In particular, the violation of the C/CP symmetry naturally arises in the two-brane universe model through the occurrence of a scalar field resulting from the splitting of the electromagnetic gauge field on each brane. The coupling constant \bar{g} describing the $\bar{n} - \bar{n}'$ transition between the antineutron and hidden antineutron sectors then differs from g . Consequently, $\bar{n} - \bar{n}'$ transitions would occur at a different rate than $n - n'$ transitions with an asymmetry allowing the current baryon-antibaryon ratio with respect of the Sakharov conditions [2, 48].

The study is organized as follows. In Section II, one provides a brief overview of the theoretical framework previously introduced [36, 44–47], and which enables the study of particle dynamics in a two-brane universe. In Section III, one shows how the electromagnetic gauge field $U(1) \otimes U(1)$ in a two-brane universe naturally replaces the $U(1)$ gauge field, and how an additional scalar field then arises. One then shows and discusses how this

* michael.sarrazin@ac-besancon.fr

field breaks the C/CP symmetry in Section IV, also introducing the interbrane coupling Hamiltonian. Next, in Section V, it is shown that the coupling constant \bar{g} between the antineutron and hidden antineutron sectors must then differ from g . Both coupling constants g and \bar{g} are naturally modified, leading to the expected conditions for baryogenesis. In section VI, from the interbrane coupling Hamiltonian, one introduces the Boltzmann equations relevant to describe the baryogenesis in a two-brane universe. The results obtained from these equations are shown and discussed in the section VII. Finally, before concluding, in Section VIII one discusses about the scalar waves that could be dark matter candidates allowing then to constrain the present model at the laboratory scale or from astrophysical data. This is an important experimental perspective since the direct experimental study of $\bar{n} - \bar{n}'$ transitions is far beyond the current technological state of the art [37–41].

II. FERMION DYNAMICS IN A TWO-BRANE UNIVERSE

Braneworld physics and cosmology can present a complex landscape of models, making their study challenging. However, over the past two decades, it has been shown [44–47] that this study can be simplified through a mathematical and physical conjecture, which has been demonstrated in various cases [45–47, 49]:

Let us consider a two-brane universe in a $(3 + N, 1)$ –bulk ($N \geq 1$). Each brane has a thickness M_B^{-1} along extra dimensions - with M_B the brane energy scale - and d is the distance between both branes in the bulk;

- **Conjecture:** *At the sub-GeV-scale, the quantum dynamics of fermions in the two-brane universe is the same as in a two-sheeted space-time $M_4 \times Z_2$ described with noncommutative geometry.*

The phenomenological discrete space-time $M_4 \times Z_2$ replaces the physical continuous $(3 + N, 1)$ –bulk ($N \geq 1$) with its two branes [45–47]. At each point along the discrete extra dimension Z_2 , there is a four-dimensional space-time M_4 endowed with its own metric. Each M_4 sheet describes each braneworld considered as being separated by a phenomenological distance $\delta = 1/g$, with g the coupling constant between fermionic sectors. g is a function against M_B , d and also the mass of the fermion under consideration [45–47]. The function can also depend on the bulk properties (i.e. dimensionality and compactification). For instance, for neutron and a $M_4 \times R_1$ bulk, one gets [46, 47]:

$$g \sim \frac{m_Q^2}{M_B} e^{-m_Q d}, \quad (1)$$

where m_Q is the mass of the quark constituents in the neutron – i.e. the mass of the quarks up and down dressed with gluons fields and virtual quarks fields such that $m_Q = m_{up} = m_{down} = 327$ MeV [50–53].

The effective $M_4 \times Z_2$ Lagrangian for the fermion dynamics in a two-brane Universe is [45–47]:

$$\mathcal{L}_{M_4 \times Z_2} \sim \bar{\Psi} (i\mathcal{D} - m) \Psi. \quad (2)$$

Labeling (+) (respectively (–)) our brane (respectively the hidden brane), one writes: $\Psi = \begin{pmatrix} \psi_+ \\ \psi_- \end{pmatrix}$ where ψ_{\pm} are the wave functions in the branes (\pm) and m is the mass of the bound fermion on a brane, here the quark constituent. The derivative operators acting on M_4 and Z_2 are $D_\mu = \mathbf{1}_{8 \times 8} \partial_\mu$ ($\mu = 0, 1, 2, 3$) and $D_5 = ig\sigma_2 \otimes \mathbf{1}_{4 \times 4}$, respectively, and the Dirac operator acting on $M_4 \times Z_2$ is defined as $\mathcal{D} = \Gamma^N D_N = \Gamma^\mu D_\mu + \Gamma^5 D_5$ where: $\Gamma^\mu = \mathbf{1}_{2 \times 2} \otimes \gamma^\mu$ and $\Gamma^5 = \sigma_3 \otimes \gamma^5$. γ^μ and $\gamma^5 = i\gamma^0\gamma^1\gamma^2\gamma^3$ are the usual Dirac matrices and σ_k ($k = 1, 2, 3$) the Pauli matrices. Eq. (2) is characteristic of fermions in noncommutative $M_4 \times Z_2$ two-sheeted space-times as introduced by other authors [54–61].

One refers to the terms proportional to g as geometrical mixing [45–47]. The present conjecture serves as a valuable tool for investigating the phenomenology of braneworlds and exploring their implications within realistic experimental settings [37–41].

In the following sections, one shows how the violation of C/CP symmetry naturally arises from the $M_4 \times Z_2$ framework, using the scalar field that emerges from the splitting of the electromagnetic gauge field. Therefore, it is necessary to consider $U(1) \otimes U(1)$ instead of $U(1)$.

III. GAUGE FIELD AND EXTRA SCALAR FIELD

In a two-brane universe, the electromagnetic field is described by the effective $U(1)_+ \otimes U(1)_-$ gauge field in the $M_4 \times Z_2$ space-time [45]. Here, $U(1)_+$ is the gauge group associated with the photon field localized on our brane, while $U(1)_-$ is the gauge group of the photon field localized on the hidden brane. This is not merely a corollary of the $M_4 \times Z_2$ description, but a demonstrated consequence when examining the low-energy dynamics of fermions in the two-brane system¹[45]. The group representation is therefore:

$$G = \text{diag} \{ \exp(-iq\Lambda_+), \exp(-iq\Lambda_-) \}. \quad (3)$$

Looking for an appropriate gauge field such that the gauge covariant derivative is $\mathcal{D}_A \rightarrow \mathcal{D} + iq\mathcal{A}$ with the following gauge transformation rule:

$$\mathcal{A}' = G\mathcal{A}G^\dagger - \frac{i}{q}G[\mathcal{D}, G^\dagger], \quad (4)$$

¹ It is noteworthy that the phenomenology of the gauge group $U(1) \otimes U(1)$ also manifests in other contexts beyond brane physics [54–63].

with q the fermion charge – one gets the most general form of the electromagnetic potential:

$$\mathcal{A} = \begin{pmatrix} \gamma^\mu A_\mu^+ & \phi \gamma^5 \\ -\phi^* \gamma^5 & \gamma^\mu A_\mu^- \end{pmatrix}. \quad (5)$$

Thanks to seminal works on noncommutative geometry by Connes, followed by other authors [54–61], attempts have been made to derive the standard model of particle physics using a two-sheeted space-time. In this context, the scalar field was associated with the Higgs field. However, in the present study, one does not consider such a hypothesis. Instead, one refers to the interpretation of the scalar field as demonstrated in our previous works, where the $M_4 \times Z_2$ approach is derived as an effective limit of a two-brane world in a continuous bulk [45]. Then, one can assume the presence of an extra dimensional component of the electromagnetic gauge field $U(1)$ in the bulk, and ϕ (see Eq. (5)) represents this additional component dressed by fluctuating fermionic fields in the bulk [45]. However, as a proof of principle, in the present model one uses the definition of the field strength used by Connes *et al.* [54–61], one sets:

$$\mathcal{F} = \{i\mathcal{D}, \mathcal{A}\} + e\mathcal{A}\mathcal{A}, \quad (6)$$

modulo the *junk* terms [54–61], with e here the electromagnetic coupling constant. The gauge field Lagrangian being defined as: $\mathcal{L} = -\frac{1}{4}\text{Tr}\{\mathcal{F}\mathcal{F}\}$, from Eq. (6) one gets [54–61]:

$$\begin{aligned} \mathcal{L} = & -\frac{1}{4}F^{+\mu\nu}F_{\mu\nu}^+ - \frac{1}{4}F^{-\mu\nu}F_{\mu\nu}^- \\ & + (\mathcal{D}_\mu h)^* (\mathcal{D}^\mu h) - \frac{e^2}{2} (|h|^2 - 2\eta^2)^2, \end{aligned} \quad (7)$$

with $F_{\mu\nu}^\pm = \partial_\mu A_\nu^\pm - \partial_\nu A_\mu^\pm$ (A_μ^\pm are the electromagnetic four-potentials on each brane (\pm)) and where the Lorenz gauge and the field transversality are imposed, and where one has set:

$$\mathcal{D}_\mu = \partial_\mu - ie (A_\mu^+ - A_\mu^-), \quad (8)$$

and [54–61]:

$$h = \sqrt{2}(\phi + i\eta), \quad (9)$$

with $\eta = g/e$. h is a scalar field obeying a “ φ^4 ” description, such that the vacuum state h_0 is characterized by:

$$h_0 = \eta\sqrt{2}e^{i\theta}, \quad (10)$$

where θ is a phase whose value reflects a symmetry breaking. For the sake of clarity, the outcomes resulting from the dynamics of h around the vacuum state h_0 are discussed in section VIII. In the following two sections, one considers the scalar field h in its vacuum state h_0 .

IV. SCALAR FIELD-INDUCED C/CP VIOLATION AND INTERBRANE COUPLING HAMILTONIAN

Writing now the two-brane Dirac equation including the gauge field from Eqs. (2), (4) and (5) one gets:

$$\begin{pmatrix} i\gamma^\mu (\partial_\mu + iqA_\mu^+) - m & ig_c\gamma^5 \\ ig_c^*\gamma^5 & i\gamma^\mu (\partial_\mu + iqA_\mu^-) - m \end{pmatrix} \Psi = 0, \quad (11)$$

with:

$$g_c = g + iq\phi_0, \quad (12)$$

here with $\phi_0 = \eta(e^{i\theta} - i)$ (see Eqs. (9) and (10)) as the scalar field is on the vacuum state. It must be underlined that in our previous work [45], the role of the scalar field was neglected – such that $g_c = g_c^* = g$ – while here one explores its consequences. It is then convenient to write g_c as:

$$g_c = \mathbf{g}e^{i\alpha}, \quad (13)$$

with:

$$\mathbf{g} = g\sqrt{1 + 2z(1+z)(1 - \sin\theta)}, \quad (14)$$

where $z = q/e$, and:

$$\tan\alpha = \frac{z \cos\theta}{1 + z(1 - \sin\theta)}. \quad (15)$$

Then, thanks to a simple phase rescaling $\Psi \rightarrow T\Psi$, with $T = \text{diag}\{e^{i\alpha/2}, e^{-i\alpha/2}\}$, one gets from Eq. (11):

$$\begin{pmatrix} i\gamma^\mu (\partial_\mu + iqA_\mu^+) - m & i\mathbf{g}\gamma^5 \\ i\mathbf{g}\gamma^5 & i\gamma^\mu (\partial_\mu + iqA_\mu^-) - m \end{pmatrix} \Psi = 0. \quad (16)$$

Now, let us consider the standard procedure for obtaining the Pauli equation from the Dirac equation in its two-brane formulation (16). By doing so, one can derive the interbrane coupling Hamiltonian for a fermion (see [36, 45]):

$$\mathcal{W} = \varepsilon \begin{pmatrix} 0 & \mathbf{u} \\ \mathbf{u}^\dagger & 0 \end{pmatrix}, \quad (17)$$

where $\varepsilon = \mathbf{g}\mu|\mathbf{A}_+ - \mathbf{A}_-|$ with \mathbf{A}_\pm the local magnetic vector potentials in each brane [36, 45], μ the magnetic moment of the fermion and \mathbf{u} a unitary matrix such that: $\mathbf{u} = i\mathbf{e} \cdot \boldsymbol{\sigma}$ with $\mathbf{e} = (\mathbf{A}_+ - \mathbf{A}_-)/|\mathbf{A}_+ - \mathbf{A}_-|$. The phenomenology related to \mathcal{W} is explored and is detailed elsewhere [36–41, 44–47]. From the Hamiltonian (17), one can show that a particle should oscillate between two states: One localized in our brane and the other localized in the hidden world [45]. While such oscillations are suppressed for charged particles [34, 36, 64], they remain possible for composite particles with neutral charge such as neutrons or antineutrons [34, 36, 64], for which

the above coupling has the same form. This could result in the disappearance [37] or reappearance of neutrons, allowing for passing-through-walls neutron experiments, which have been conducted in the last decade [38–41]. Such phenomena would appear as a baryon number violation.

The interbrane coupling Hamiltonian \mathcal{W} for the anti-fermion can be obtained through the charge conjugation $q \rightarrow -q$ in Eqs. (17) and (14). One labels $\bar{\mathbf{g}}$ the coupling constant between the visible and the hidden sectors for the anti-fermion. For the antiparticle the sign change $\mu \rightarrow -\mu$ due to the charge conjugation can be effectively eliminated through a relevant phase rescaling in Eq. (17). It is not the case for the coupling constant. When $\phi = 0$, we have $\mathbf{g} = g$, and the antiparticle also exhibits $\bar{\mathbf{g}} = g$. However, in the case where $\phi \neq 0$, one finds $\mathbf{g} \rightarrow \bar{\mathbf{g}} \neq \mathbf{g}$ (with $\bar{\mathbf{g}}, \mathbf{g} > 0$), and this disparity cannot be canceled: the interbrane coupling magnitude differs between the particle and the antiparticle. Then, the presence of a scalar field in the two-brane universe breaks the symmetry between $\bar{\mathbf{g}}$ and \mathbf{g} . It must be underlined that such an asymmetry would be hidden from us in our visible world, except for experiments involving neutron and antineutron disappearance and/or reappearance [38–41]. Nevertheless, in section VIII, one will suggest a way to experimentally constrain our scenario by testing the existence of scalar bosons related to the scalar field.

V. NEUTRON AND ANTINEUTRON INTERBRANE COUPLING CONSTANTS

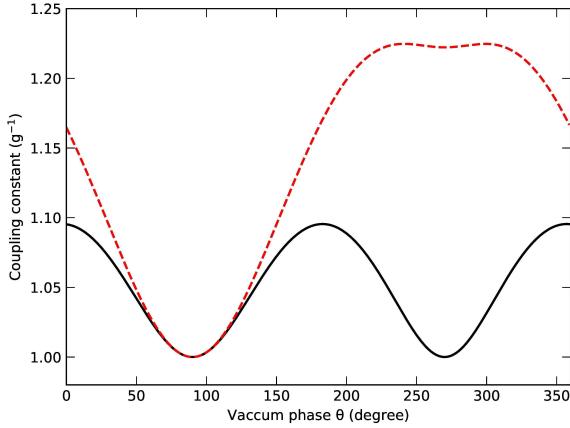


FIG. 1. (Color online). Normalized coupling constant for neutron \mathbf{g}/g (black line) and antineutron $\bar{\mathbf{g}}/g$ (red dashed line) against the scalar field phase θ in the vacuum state.

The two-brane Dirac equation (16) can be fundamentally derived [46, 47] to describe quarks within baryons (or mesons). But, Eq. (14) cannot be directly applied to characterize the neutron [46, 47] or the antineutron as they are not pointlike particles. In order to address this issue, the well-known quark constituent model [50–53] is

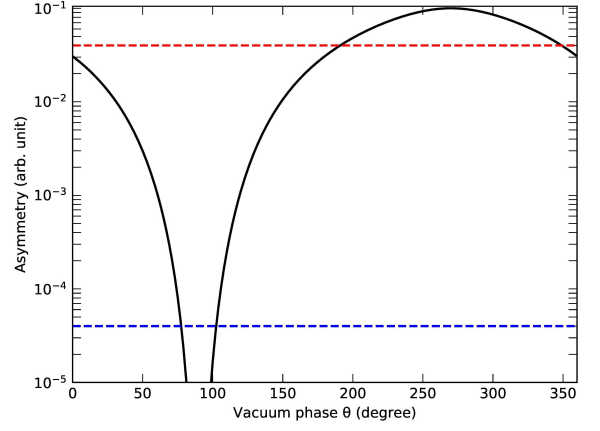


FIG. 2. (Color online). Asymmetry $\delta = \Delta\mathbf{g}/\mathbf{g}$ against the scalar field phase θ in the vacuum state. Upper red dashed line: upper limit on the asymmetry compatible with baryogenesis as shown in section VII (see Eq. (50)). Lower blue dashed line: lower limit compatible with baryogenesis (section VII, Eq. (50)).

pursued as outlined elsewhere [46, 47]. In this context, assuming that \mathbf{g} (respectively $\hat{\mu}_n$) represents the coupling constant (respectively, the magnetic moment operator) of the neutron, the quark constituent model [50–53] is employed and one gets:

$$\mathbf{g}\hat{\mu}_n = \sum_q \hat{\mu}_q \mathbf{g}_q, \quad (18)$$

where \mathbf{g}_q (respectively $\hat{\mu}_q$) refers to the coupling constant (respectively the magnetic moment operator) of each quark constituting the neutron with $\hat{\mu}_n = \sum_q \hat{\mu}_q$.

The magnetic moment of the neutron μ_n is then calculated by taking the expectation value of the operator $\hat{\mu}_n$, and one gets [50]:

$$\mu_n = \langle n, \uparrow | \hat{\mu} | n, \uparrow \rangle = \frac{4}{3}\mu_d - \frac{1}{3}\mu_u, \quad (19)$$

where – without loss of generality – one has considered the neutron with spin up such that [50]:

$$|n, \uparrow\rangle = \frac{1}{\sqrt{18}} (-2 |d, \uparrow\rangle |d, \uparrow\rangle |u, \downarrow\rangle + |d, \uparrow\rangle |d, \downarrow\rangle |u, \uparrow\rangle + |d, \downarrow\rangle |d, \uparrow\rangle |u, \uparrow\rangle + \text{permutations}), \quad (20)$$

with $|u, \uparrow\rangle$ and $|d, \uparrow\rangle$ the quark up and the quark down wave-functions respectively, either with spin up \uparrow or down \downarrow . Also, one gets:

$$\mu_u = \frac{2}{3} \frac{e\hbar}{2m_u} \text{ and } \mu_d = -\frac{1}{3} \frac{e\hbar}{2m_d}. \quad (21)$$

Using $m_{up} = m_{down} = m_Q = 327 \text{ MeV}$ [50–53], one obtains [50]:

$$\mu_n = -\frac{2}{3} \frac{e\hbar}{2m_Q}. \quad (22)$$

Doing the same with $g\hat{\mu}$, one deduces from Eq. (18):

$$\mathfrak{g}\mu_n = \frac{4}{3}\mathfrak{g}_d\mu_d - \frac{1}{3}\mathfrak{g}_u\mu_u, \quad (23)$$

and using Eq. (22) one finally gets:

$$\mathfrak{g} = \frac{2}{3}\mathfrak{g}_d + \frac{1}{3}\mathfrak{g}_u. \quad (24)$$

From Eqs. (14) and (24), one deduces the explicit expression:

$$\frac{\mathfrak{g}}{g} = \frac{2}{9}\sqrt{5+4\sin\theta} + \frac{1}{9}\sqrt{29-20\sin\theta}. \quad (25)$$

Doing the same for the antineutron, one gets:

$$\frac{\bar{\mathfrak{g}}}{g} = \frac{2}{9}\sqrt{17-8\sin\theta} + \frac{1}{9}\sqrt{5+4\sin\theta}. \quad (26)$$

In the following, one defines the asymmetry of the inter-brane coupling constants of the neutron and antineutron as:

$$\delta = \frac{\Delta\mathfrak{g}}{\mathfrak{g}} = \frac{|\bar{\mathfrak{g}} - \mathfrak{g}|}{\bar{\mathfrak{g}} + \mathfrak{g}}, \quad (27)$$

and one gets:

$$\delta = \frac{|\sqrt{5+4\sin\theta} + \sqrt{29-20\sin\theta} - 2\sqrt{17-8\sin\theta}|}{3\sqrt{5+4\sin\theta} + \sqrt{29-20\sin\theta} + 2\sqrt{17-8\sin\theta}}, \quad (28)$$

which does not depend on the expression of g and therefore, not on the bulk dimensionality.

In Fig. 1, the normalized coupling constants for the neutron, \mathfrak{g}/g , and the antineutron, $\bar{\mathfrak{g}}/g$, are illustrated against the scalar field phase θ in the vacuum state. Figure 2 displays the asymmetry $\Delta\mathfrak{g}/\mathfrak{g}$ plotted against θ . The upper red dashed line represents the upper limit on the asymmetry compatible with baryogenesis as shown in section VII (see Eq. (50)). The lower blue dashed line represents the lower limit compatible with baryogenesis (section VII, Eq. (50)). The values of θ that are compatible with baryogenesis span a range of 177 degrees. In terms of symmetry breaking, there is a very high probability – almost a 1 in 2 chance – that symmetry breaking can promote baryogenesis as described in the next sections VI and VII.

VI. BARYON PHENOMENOLOGY IN THE EARLY TWO-BRANE UNIVERSE

Usually, the Boltzmann transport equation [65, 66] leads to the Lee-Weinberg equations [67] that govern the density of relic particles in the expanding Universe. The

density of baryons n_B (respectively antibaryons $n_{\bar{B}}$) thus obeys to [65, 66]:

$$\partial_t n_B + 3Hn_B = -\langle\sigma_a v\rangle\left(n_B n_{\bar{B}} - n_{B,eq} n_{\bar{B},eq}\right), \quad (29)$$

with H the Hubble parameter, σ_a the baryon-antibaryon annihilation cross-section, v the relative velocity between particles, and $\langle\cdots\rangle$ the thermal average at temperature T . Quantities $n_{B,eq}$ and $n_{\bar{B},eq}$ are at the thermal equilibrium and are described by the Fermi-Dirac statistics. Without baryon-antibaryon asymmetry, one would have $n_B = n_{\bar{B}}$, and the same expression would occur for antibaryons through the $n_B \leftrightarrow n_{\bar{B}}$ substitution. Under such conditions, particles would simply annihilate until the expansion of space froze the process by reducing the probability of collision between particles and antiparticles. Then, baryons and antibaryons would have the same density in the Universe (there would be no asymmetry) but lower by many orders of magnitude than the current observed values. However, the current imbalance in the observed Universe between baryons and antibaryons – with a large photon population – suggests an early asymmetry. One actually observes [3]:

$$Y_B - Y_{\bar{B}} = (8.8 \pm 0.6) \times 10^{-11} \quad (30)$$

where $Y_X = n_X/s$ is the comoving particle density, i.e. the particle density n_X related to the entropy density s , itself proportional to the photon population [65, 66]. As the temperature of the Universe decreased, a baryonic asymmetry could have precluded the complete annihilation of all matter and antimatter, resulting in a very small excess of matter over antimatter. The baryogenesis process supposes that the three Sakharov conditions [48] are satisfied: Baryon number violation, C-symmetry and CP-symmetry violation, and interactions out of thermal equilibrium. Currently, C/CP violation processes known in physics are too weak in magnitude to explain baryogenesis, and solutions are expected from attempts to build a grand unified theory. However, for now, the origin of the imbalance between matter and antimatter is still unknown, despite the existence of many hypotheses [2–4, 68].

In sections III, IV and V, it is underlined that neutron and antineutron could be the portal inducing the baryogenesis right after the phase transition from quark-gluon plasma to hadron gas (QGPHG). Keeping the Sakharov conditions in mind, we propose to discuss the magnitude of the asymmetry between \mathfrak{g} and $\bar{\mathfrak{g}}$ and its consequences in a baryogenesis scenario. Between the QGPHG transition ($T_0 \approx 160$ MeV) and the end of baryon-antibaryon annihilation ($T \approx 20$ MeV), we need to explain the similarities of the temperatures in each brane, a condition necessary as shown later. This could be possible if the branes had collided during the initial stage of the Big Bang, regardless of the underlying mechanisms during the collision of the branes [22–33].

Let us consider matter (or antimatter) exchange between two branes: the one corresponding to our visible

Universe and a hidden one. The process is described through the Hamiltonian (17) added to a Hamiltonian \mathcal{H}_0 describing the neutron (or antineutron) in each brane such that $\mathcal{H} = \mathcal{H}_0 + \mathcal{W}$, with $\mathcal{H}_0 = \text{diag}\{E_+, E_-\}$ and $E_{\pm} = E_{0,\pm} + V_{F,\pm}$, where $E_{0,\pm}$ are the eigenenergies of the particle in vacuum either in its visible state or its hidden state due to the gravitational potentials of each brane, and $V_{F,\pm}$ are the Fermi potentials of the materials through which the particle travels [38, 41]. The visible or hidden states of matter (or antimatter) are quantum states, but not eigenstates of (17). Therefore, the Lindblad equation formalism [69] is necessary to describe the dynamics of quantum states that change a visible neutron n into a hidden one n' (or a visible antineutron \bar{n} into a hidden one \bar{n}') – and vice versa – as a result of interactions with many scatterers X (i.e. $n + X \leftrightarrow n' + X$). This equation extends the Liouville-Von Neumann equation related to the density matrix ρ – and allows the study of the evolution of a quantum system (the neutron or antineutron) interacting with two environments that are not in thermal equilibrium [69], i.e., a set of scatterers X in our brane and a set of scatterers X' in the hidden brane. For the two-brane Universe, the Lindblad equation can be written as:

$$\partial_t \rho + \frac{3}{2} \{H, \rho\} = i[\rho, \mathcal{H}] + L(\rho), \quad (31)$$

where $\{A, B\} = AB + BA$ defines the anticommutator,² with $H = \text{diag}\{H_+, H_-\}$ and H_{\pm} the Hubble parameters in each brane. The Lindblad operator $L(\rho)$ is defined as [69]:

$$L(\rho) = \sum_m \Gamma_m \left(C_m \rho C_m^\dagger - \frac{1}{2} \{ \rho, C_m^\dagger C_m \} \right), \quad (32)$$

where C_m ($m = \pm$) are the jump operators describing the wave function reduction process either into the visible or into the hidden branes when the system interacts with its environment.³ Then, Γ_+ (respectively Γ_-) describes the collisional rate between the neutron (or antineutron) and the environment in the brane $+$ (respectively in the brane $-$) when it is assumed to be in this brane. In the following, T is the temperature in our visible braneworld and T' in the hidden braneworld, such that:

$$\kappa = \frac{T}{T'}, \quad (33)$$

where κ is a constant parameter. Setting σ the usual elastic cross-section $\sigma = \sigma(n + X \rightarrow n + X)$, one gets:

$\Gamma_+ = \langle \sigma v \rangle n_X$ and $\Gamma_- = \langle \sigma v \rangle' n_{X'}$,⁴ where [70]:

$$\begin{aligned} \langle \sigma v \rangle &= \int \int d^3 \mathbf{v}_1 d^3 \mathbf{v}_2 f_T(\mathbf{v}_1) f_T(\mathbf{v}_2) \sigma |\mathbf{v}_1 - \mathbf{v}_2| \\ &= \frac{x^{3/2}}{2\sqrt{\pi}} \int_0^\infty dv v^2 e^{-xv^2/4} \sigma v, \end{aligned} \quad (34)$$

with $x = m/T$ the usual parameter [65, 66] used to follow the primordial particle dynamics, and m a mass reference, here equals to the typical mass of the nucleon: 939 MeV/c². One also uses $x' = m/T' = \kappa x$.

Setting:

$$\rho = \begin{pmatrix} \rho_+ & x - iy \\ x + iy & \rho_- \end{pmatrix}, \quad (35)$$

Eq. (31) for unpolarized fermions becomes:

$$\begin{cases} \partial_t \rho_+ = -3H_+ \rho_+ + 2\varepsilon y \\ \partial_t \rho_- = -3H_- \rho_- - 2\varepsilon y \\ \partial_t x = -(3H + \Gamma)x - \Delta E y \\ \partial_t y = -(3H + \Gamma)y + \Delta E x - \varepsilon(\rho_+ - \rho_-) \end{cases} \quad (36)$$

with $\Delta E = E_+ - E_-$, $H = (H_+ + H_-)/2$ and $\Gamma = (\Gamma_+ + \Gamma_-)/2$ and where ΔE , Γ and ε can depend on time. Here, due to the isotropy and the homogeneity of the Universe in both branes, and due to the strong collisional dynamics:⁵ $\Gamma \gg H > \Delta E$. This allows for the stationary phase approximation [38, 40, 41]: $\partial_t x \approx \partial_t y \approx 0$, and the system (36) can be conveniently recast as:

$$\begin{cases} \partial_t n_n + 3H_+ n_n = -\gamma(n_n - n_{n'}) \\ \partial_t n_{n'} + 3H_- n_{n'} = -\gamma(n_{n'} - n_n) \end{cases}, \quad (37)$$

with γ the neutron transition rate between branes such that:

$$\gamma = \frac{2(3H + \Gamma)\varepsilon^2}{(3H + \Gamma)^2 + \Delta E^2}. \quad (38)$$

and where one used: $n_n = n_0 \rho_+$ and $n_{n'} = n_0 \rho_-$ with n_0 the global neutron population in the two-brane Universe [38, 41]. Since $\Gamma \gg H > \Delta E$, one gets: $\gamma \sim 2\varepsilon^2/\Gamma$.

During the period of interest, the coupling parameter ε depends only on the typical amplitude A of the magnetic vector potentials related to primordial magnetic fields [71], then:⁶ $A = A_0(x_0/x)$, with $A_0 \approx 4.0 \times 10^8$ T.m

⁴ $\langle \dots \rangle'$ is the thermal average at T' .

⁵ The Fermi potential writes as $V_F = (2\pi\hbar^2/m)bn_X$ with m the neutron mass and b the scattering length on a free nucleon ($b \approx 0.73$ fm). Then, $\Gamma \gg V_F$ leads to $\langle \sigma v \rangle \gg (2\pi\hbar/m)b$ which is verified in the present work.

⁶ The magnetic vector potential is given by $A_0 \sim B_0 L_0$ with $B_0 \approx 10^4$ T the field strength at the QCD phase transition time (i.e. at T_0) [72] and L_0 the maximal coherence length of the magnetic field at the same epoch, i.e. $L_0 \sim H^{-1}$ [72] with H the Hubble parameter.

² The term $(3/2)\{H, \rho\}$ arises from the covariant derivatives in the Dirac equation for a universe with two space-time sheets (or branes) endowed with their own tensor metric: $g_{\pm, \mu\nu}^{(4)} = \text{diag}(1, -a_{\pm}^2(t), -a_{\pm}^2(t), -a_{\pm}^2(t))$ with scale factors a_{\pm} such that $H_{\pm} = (\partial_t a_{\pm})/a_{\pm}$ are the Hubble parameters in each brane.

³ $C_+ = \text{diag}\{1, 0\}$ and $C_- = \text{diag}\{0, 1\}$.

the typical amplitude at $T = T_0$, i.e. at the QGPHG transition [71, 72]. Then:

$$\varepsilon = \varepsilon_0 \frac{x_0}{x} \quad (39)$$

with⁷ $\varepsilon_0 = \mathbf{g}\mu_n A_0$.

A set of equations similar to Eq. (37) can be derived for antineutrons – with $n_{\bar{n}}$ and $n_{\bar{n}'}$ – but where $\bar{\gamma} = 2\bar{\varepsilon}^2/\bar{\Gamma}$ – with $\bar{\varepsilon}_0 = \bar{\mathbf{g}}\mu_{\bar{n}} A_0$ and where $\bar{\Gamma}$ will be conveniently defined in details below.

The system of equations (37) now allows us to extend Eq. (29). The right-hand side of equation (29) for neutrons (or antineutrons) can be written for both brane + and brane – and must be added to the right-hand sides of the two expressions in system (37) for each brane.

In the period of interest, the Universe is composed of various baryons, mesons, leptons, and neutrinos. However, we consider that the dynamics of nucleons primarily depends on their equilibrium with the lightest leptons and related neutrinos. Electrons, positrons, neutrinos, and antineutrinos are relativistic and in thermal equilibrium with the photon bath. Therefore: $n_{e^-} = n_{e^-,eq} = n_{e^+} = n_{e^+,eq} = n_{l,eq}$ (the same is true for the hidden brane). At equilibrium, above the threshold temperature of the electron-positron plasma, the populations of protons and neutrons follow: $n_{n,eq} = n_{p,eq} (m_n/m_p)^{3/2} \exp(-\Delta m/T)$ (with $\Delta m = m_n - m_p$) as neutrons contribute to the protons population mainly through $n + e^+ \rightarrow p + \bar{\nu}$ and as protons contributes to the neutrons population through $p + e^- \rightarrow n + \nu$. During the period of interest, as a fair approximation, we assume: $n_{p,eq} = n_{n,eq}$ and $n_{\bar{p},eq} = n_{\bar{n},eq}$ and the same for the hidden brane, but also $n_n = n_p = (1/2)n_B$, $n_{\bar{n}} = n_{\bar{p}} = (1/2)n_{\bar{B}}$, $n_{n'} = n_{p'} = (1/2)n_{B'}$ and $n_{\bar{n}'} = n_{\bar{p}'} = (1/2)n_{\bar{B}'}$. Writing then the system (37) including the Lee-Weinberg equations for each particle species – and for particles and antiparticles – and assuming the above hypothesis, one easily obtains:

$$\begin{aligned} \frac{dY_B}{dx} &= -\langle \sigma_{B\bar{B},a} v \rangle \eta \frac{s}{Hx} (Y_B Y_{\bar{B}} - Y_{B,eq} Y_{\bar{B},eq}) \\ &\quad - (1/2) \frac{\gamma \eta}{Hx} (Y_B - Y_{B'}), \end{aligned} \quad (40)$$

$$\begin{aligned} \frac{dY_{\bar{B}}}{dx} &= -\langle \sigma_{B\bar{B},a} v \rangle \eta \frac{s}{Hx} (Y_B Y_{\bar{B}} - Y_{B,eq} Y_{\bar{B},eq}) \\ &\quad - (1/2) \frac{\bar{\gamma} \eta}{Hx} (Y_{\bar{B}} - Y_{\bar{B}'}), \end{aligned} \quad (41)$$

⁷ Since $\varepsilon = \mathbf{g}\mu_n |\mathbf{A}_+ - \mathbf{A}_-|$, one considers that: $A_+ = A_0(x_0/x)$ and $A_- = A_0(x_0/x')$ and the fact that \mathbf{A}_+ and \mathbf{A}_- should have different orientations in various domains of the early Universe. Then, one uses $\varepsilon = \mathbf{g}\mu_n \langle |\mathbf{A}_+ - \mathbf{A}_-| \rangle$ with $\langle |\mathbf{A}_+ - \mathbf{A}_-| \rangle$ the averaged value over all the possible relative directions between \mathbf{A}_+ and \mathbf{A}_- . One shows: $\langle |\mathbf{A}_+ - \mathbf{A}_-| \rangle = A_+(2/\pi) (1 + 1/\kappa) E\left(\frac{4\kappa}{(1+\kappa)^2}\right) \sim A_+$ for $1 < \kappa < 3$. $E(x)$ is the complete elliptic integral of the second kind.

$$\begin{aligned} \frac{dY_{B'}}{dx} &= -\langle \sigma_{B\bar{B},a} v \rangle' \eta' \frac{\kappa s'}{H'x'} (Y_{B'} Y_{\bar{B}'} - Y_{B',eq} Y_{\bar{B}',eq}) \\ &\quad - (1/2) \frac{\gamma \kappa \eta'}{H'x'} (Y_{B'} - Y_B), \end{aligned} \quad (42)$$

$$\begin{aligned} \frac{dY_{\bar{B}'}}{dx} &= -\langle \sigma_{B\bar{B},a} v \rangle' \eta' \frac{\kappa s'}{H'x'} (Y_{B'} Y_{\bar{B}'} - Y_{B',eq} Y_{\bar{B}',eq}) \\ &\quad - (1/2) \frac{\bar{\gamma} \kappa \eta'}{H'x'} (Y_{\bar{B}'} - Y_{\bar{B}}), \end{aligned} \quad (43)$$

where we have introduced the comoving particle densities: $Y_B = n_B/s$, $Y_{\bar{B}} = n_{\bar{B}}/s$, $Y_{B'} = n_{B'}/s'$ and $Y_{\bar{B}'} = n_{\bar{B}'}/s'$ with s and s' the entropy densities in each brane. We have also proceeded to the variable changing $t \rightarrow x$ such that $(H_+, H_-) \rightarrow (H, H')$ (see Eq. 46) with the relations [65, 66]: $dx/dt = Hx/\eta$ and $dx'/dt = H'x'/\eta'$ in each brane, where:

$$\eta = 1 - \frac{x}{3q_*} \frac{dq_*}{dx}, \quad (44)$$

with q_* the effective number of degrees of freedom defined for the entropy density such that [65, 66]:

$$s = \frac{2\pi^2}{45} m^3 q_* x^{-3}. \quad (45)$$

While η is often close to 1 during most of the radiation era, it is not the case shortly after the QGPHG transition as pions and muons annihilate between 160 MeV and 100 MeV leading then to a fast change of q_* against x . In the same way, since the period of interest is radiatively-dominated, the Hubble parameter is defined through [65, 66]:

$$H = \frac{2\pi\sqrt{\pi}}{3\sqrt{5}} \frac{m^2}{M_P} g_*^{1/2} x^{-2}, \quad (46)$$

with g_* the effective number of degrees of freedom defined for the energy density, and where M_P is the Planck mass. Both functions g_* and q_* can be fitted from exact computations [73] and one can set $g_* = q_*$ [65, 66, 73]. The equilibrium state of the comoving particle densities is defined as [65, 66]:

$$Y_{X,eq} = \frac{45}{2\pi^4} \sqrt{\frac{\pi}{8}} \frac{g_X}{q_*} x^{3/2} e^{-x}, \quad (47)$$

In the above equations (40) to (43), $\langle \sigma_{B\bar{B},a} v \rangle$ and $\langle \sigma_{B\bar{B},a} v \rangle'$ appear as the average rate of baryon-antibaryon annihilation with: $\sigma_{B\bar{B},a} = (1/4) (\sigma_{n\bar{n},a} + \sigma_{p\bar{p},a} + \sigma_{n\bar{p},a} + \sigma_{p\bar{n},a})$. One also defines:

$$\begin{aligned} 2\Gamma &= \langle \sigma_{BB} v \rangle s Y_B + \langle \sigma_{B\bar{B}} v \rangle s Y_{\bar{B}} \\ &\quad + \langle \sigma_{BB} v \rangle' s' Y_{B'} + \langle \sigma_{B\bar{B}} v \rangle' s' Y_{\bar{B}'}, \end{aligned} \quad (48)$$

and

$$2\bar{\Gamma} = \langle \sigma_{B\bar{B}} v \rangle s Y_B + \langle \sigma_{BB} v \rangle s Y_{\bar{B}} \quad (49)$$

$$+ \langle \sigma_{B\bar{B}} v \rangle' s' Y_{B'} + \langle \sigma_{BB} v \rangle' s' Y_{\bar{B}'},$$

with $\sigma_{BB} = (1/2)(\sigma_{np} + \sigma_{nn})$ and $\sigma_{B\bar{B}} = (1/2)(\sigma_{n\bar{p}} + \sigma_{n\bar{n}})$.⁸ Equations (40) to (43) are stiff equations. They have no analytical solutions, but they can be solved numerically by using a linear multistep method based on the backward differentiation formula (BDF) approach.⁹ The results of computations are shown and discussed in the next section.

VII. RESULTS AND DISCUSSION

In the following, one sets $M_B = M_P$ following recent bounds [40, 41, 46].

Figure 3 shows the behaviors of the comoving densities Y_B , $Y_{\bar{B}}$, $Y_{B'}$ and $Y_{\bar{B}'}$ for $\kappa = 1.1$ (i.e. T' is lower than T by 9.1%), with coupling but without asymmetry ($\delta = 0$). Y_B and $Y_{\bar{B}}$ (respectively $Y_{B'}$ and $Y_{\bar{B}'}$) in the visible brane (respectively in the hidden brane) are indistinguishable. For the sake of comparison, one shows the comoving densities for uncoupled branes (see caption), which are the expected solutions of Eq.(29). Although Y_B and $Y_{B'}$ (or $Y_{\bar{B}}$ and $Y_{\bar{B}'}$) initially have different dynamics due to different temperatures in each brane, when $x \approx 5$ all the densities converge to share the same behavior. This describes the thermalization of the two branes, which occurs due to their coupling through neutron and antineutron exchanges. However, the lack of asymmetry (i.e. $\bar{g} = g = g$) cannot lead to baryogenesis.

In figure 4, all the Sakharov conditions are present: the coupling between both branes leads to baryon number violation, the two branes are not in thermal equilibrium (here $\kappa = 1.1$), and an asymmetry resulting in C/CP violation is introduced (in the present example $\delta = 4.06 \times 10^{-4}$, see Eq. (27) in section V). Such conditions lead to baryogenesis and the current asymmetry between baryons and antibaryons.

Figure 4 provides an explanation of the baryon-antibaryon asymmetry mechanism. Early after QGPHG transition (before $x = 10$), due to C/CP violation, the swapping of antineutrons towards another brane is enhanced compared to neutrons. Since the hidden brane has a lower temperature than the visible brane, the net balance from the matter-antimatter exchange between both branes promotes a decrease in antineutrons in our

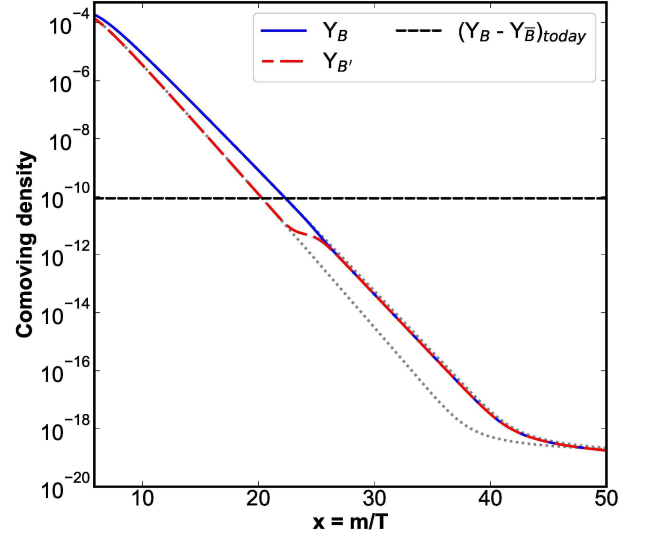


FIG. 3. (Color online). Comoving densities Y_B (superimposed with $Y_{\bar{B}}$) and $Y_{B'}$ (superimposed with $Y_{\bar{B}'}$) against x for two coupled braneworlds but with no asymmetry ($\delta = 0$) and for $\kappa = 1.1$. Upper (respectively lower) gray dotted line corresponds to Y_B and $Y_{\bar{B}}$ (respectively to $Y_{B'}$ and $Y_{\bar{B}'}$) when branes are uncoupled. All the curves are superimposed when $\kappa = 1$ and without coupling (not shown). Black dashed line is the current asymmetry given by Eq. (30).

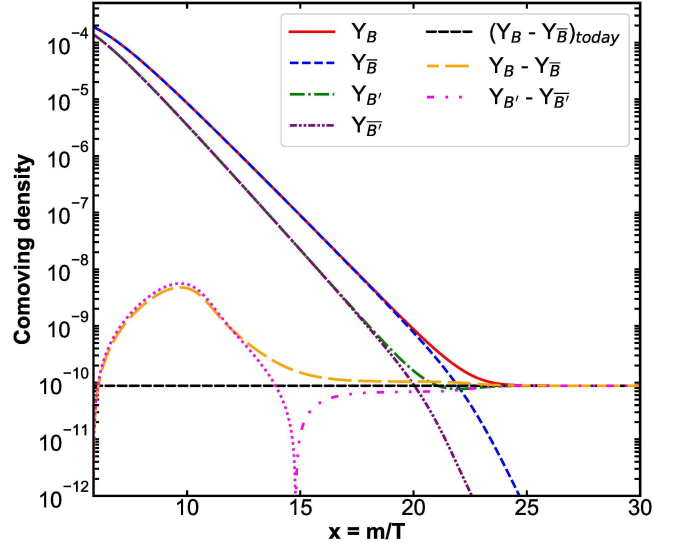


FIG. 4. (Color online). Comoving densities Y_B , $Y_{\bar{B}}$, $Y_{B'}$ and $Y_{\bar{B}'}$ against x with $\kappa = 1.1$, and a coupling between the two braneworlds with an asymmetry $\delta = 4.06 \times 10^{-4}$. Orange dashed line is the difference between populations of baryons and antibaryons. Pink line is the difference between populations of hidden baryons and hidden antibaryons. The pink dash-dot-dotted is for $Y_{B'} - Y_{\bar{B}'} > 0$, while the pink dotted line is for the opposite. Black dashed line is the current asymmetry given by Eq. (30).

⁸ Cross-sections for baryon interactions can be fitted using: $\sigma = \sigma_0 + \alpha c/v + \beta c^2/v^2$ with parameters obtained for literature [74–78], with: $\langle \sigma v \rangle = (4/\sqrt{\pi}) c \sigma_0 / \sqrt{x} + \alpha c + (\beta c / \sqrt{\pi}) \sqrt{x}$.

⁹ The ODE system under consideration is solved with a Python code using the BDF mode of the function `solve_ivp` of the SciPy module (<https://scipy.org>).

brane and an increase in the hidden brane. As a result, and due to the neutron-proton equilibrium (and

the antineutron-antiproton equilibrium) the antibaryon content decreases in our brane while the baryon content tends to dominate (as shown by the orange dashed line). In contrast, in the hidden brane the antibaryon content increases while the baryon content tends to decrease (see pink dotted line).

In a late time after the QGPHG transition (after $x = 10$), as soon as the baryonic matter widely dominates the content of our visible brane, and due to a higher temperature than in the hidden brane, baryons from our brane feed the hidden brane, allowing for annihilation of antibaryons until the matter-antimatter ratios reach the same values in both branes (pink dash-dot-dotted and orange dashed line after $x = 15$).

It should be noted that a positive asymmetry ($\delta > 0$) favors a two-brane Universe dominated by baryons, while an opposite asymmetry ($\delta < 0$) leads to a Universe dominated by antibaryons in a comparable but reversed proportion (not shown). Also, for $\kappa < 1$, the roles of the visible and hidden brane are simply reversed.

Figure 5 shows the magnitude of C/CP-violation δ (see Eq. (27) in section V) against κ , which determines the value of $Y_B - Y_{\overline{B}}$ observed today (see Eq. 30). For $\kappa = 1$ and $\kappa \gtrsim 3$, no value of δ can account for the observed imbalance between baryons and antibaryons. However, a wide range of conditions allows for the present baryon-antibaryon asymmetry with:

$$4 \times 10^{-5} < \delta < 4 \times 10^{-2}, \quad (50)$$

values that are easily reachable according to the properties of the scalar field discussed in the previous sections III to V.

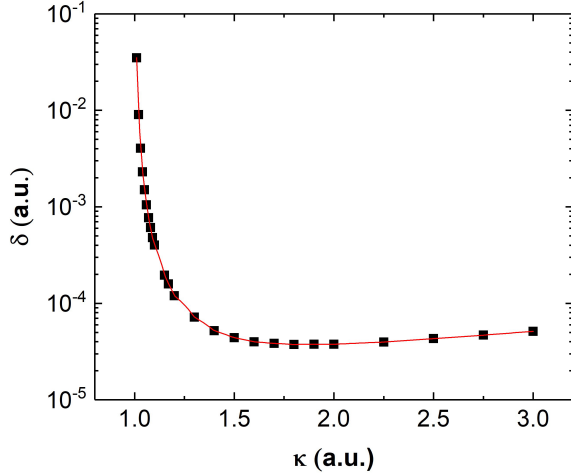


FIG. 5. (Color online). Magnitude of the asymmetry δ against κ inducing the imbalance between baryons and antibaryons observed today.

The dynamics of leptogenesis is driven by baryogenesis in order to maintain thermodynamic balance. As $Y_{p,eq} \approx Y_{n,eq}$, the neutron density decreases due to matter exchange between branes, which causes the proton

population to also decrease in order to restore equilibrium. Therefore, $Y_p = Y_n$. This occurs through proton-electron capture, which is thermodynamically favored. As a result, the electron density also decreases while the neutrino density increases. One gets: $Y_{e-} = Y_{e-,eq} - (Y_{n,eq} - Y_n)$ and $Y_\nu = Y_{\nu,eq} + (Y_{n,eq} - Y_n)$. The same process occurs for antiparticles, but antiproton-positron capture is favored. This causes the positron density to decrease while the antineutrino density increases. One gets: $Y_{e+} = Y_{e+,eq} - (Y_{\overline{n},eq} - Y_{\overline{n}})$ and $Y_{\overline{\nu}} = Y_{\overline{\nu},eq} + (Y_{\overline{n},eq} - Y_{\overline{n}})$.

By comparing the particle and antiparticle populations, one deduces: $Y_{e-} - Y_{e+} = (1/2)(Y_B - Y_{\overline{B}})$ and $Y_\nu - Y_{\overline{\nu}} = -(1/2)(Y_B - Y_{\overline{B}})$. This means that $Y_L - Y_{\overline{L}} = 0$, i.e. the global leptonic number is zero. Furthermore, positrons and antiprotons will be annihilated in such a way that each remaining proton charge is compensated by an electron charge, thereby maintaining the global neutrality of the Universe.

VIII. SCALAR WAVES AND DARK MATTER

In section IV, it has been underlined that only experiments involving antineutron disappearance and/or reappearance could allow to rise the antineutron versus neutron asymmetry. The state of the art of this kind of experiment [37–41] for the neutron requires nuclear reactors, thus implying there is no hope for convincing experiments using antineutrons. Anyway, one needs for other experimental constraints on the model introduced in the present work. It is then relevant to deepen the analysis about the fluctuations of the field h in the model using the definition of the field strength given by Eq. (6). In particular, one are going to show that the related scalar waves could allow to set constraints on the present model and could be dark matter candidates.

From the gauge transformation rule (4) the electromagnetic vector potentials follow the usual transformation rule:

$$A_\mu^{\pm'} = A_\mu^\pm + \partial_\mu \Lambda_\pm, \quad (51)$$

and from the definition of the field h (see Eq. (9)), one notes that field h should follow the gauge transformation rule:

$$h' = h \exp(i e (\Lambda_+ - \Lambda_-)). \quad (52)$$

One introduces the auxiliary fields (φ, ξ) to describe the fluctuations of h around the vacuum state h_0 , such that:

$$h = \sqrt{2} (\eta + \varphi/2) e^{i\theta} e^{i\xi/(2\eta)}. \quad (53)$$

Using Eq. (53), the gauge covariant derivative (8) of h in the Lagrangian (7) becomes:

$$\begin{aligned} \mathcal{D}_\mu h = & \sqrt{2} e^{i\theta} e^{i\xi/(2\eta)} \left(\frac{1}{2} (\partial_\mu \varphi) \right. \\ & \left. + i (\eta + \varphi/2) \left(\frac{1}{2\eta} (\partial_\mu \xi) - e (A_\mu^+ - A_\mu^-) \right) \right). \end{aligned} \quad (54)$$

The Goldstone boson field ξ can be eliminated through the Brout-Englert-Higgs-Hagen-Guralnik-Kibble mechanism [79–81]. Then, using the Lagrangian (7) and applying the usually devoted gauge transformation [79–81] with Λ_+ and Λ_- such that:

$$\Lambda_+ - \Lambda_- = -\frac{1}{2\eta e}\xi, \quad (55)$$

one gets the effective Lagrangian:

$$\begin{aligned} \mathcal{L}_{eff} \sim & -\frac{1}{4}F^{+\mu\nu}F_{\mu\nu}^+ - \frac{1}{4}F^{-\mu\nu}F_{\mu\nu}^- \\ & + \frac{1}{2}m_\varphi^2 (A_\mu^+ - A_\mu^-) (A^{\mu+} - A^{\mu-}) \\ & + \frac{1}{2}(\partial_\mu\varphi)(\partial^\mu\varphi) - \frac{1}{2}m_\varphi^2\varphi^2 \\ & + \left(\frac{1}{2}e^2\varphi^2 + 2ge\varphi\right) (A_\mu^+ - A_\mu^-) (A^{\mu+} - A^{\mu-}), \end{aligned} \quad (56)$$

with:

$$m_\varphi = 2g. \quad (57)$$

That implies a broken symmetry such that the phase of h (i.e. θ) does not vary against space and time and is an unknown parameter of the present model. Small perturbations φ ($\varphi \ll \eta$) around the vacuum state do not affect the baryogenesis model and correspond to a scalar field propagating along the branes with a mass m_φ .

Eq. (56) implies that the photon fields of each brane and the scalar field are coupled to each other. One will not discuss here the coupling between electromagnetic fields, which is left to future work. The photon also gets a mass equals to m_φ . The fact the photon is endowed with a mass implies strong constraints on g from the photon mass bounds obtained from various laboratory experiments or from astrophysical observations (see [82] and references within). Currently, one would get $g \lesssim 10^{-18}$ eV [82]. Although this current days value seems too small to allow for baryogenesis in our model, the magnitude of g could have been significantly larger at the baryogenesis epoch. Indeed, from Eq. (1), and assuming an ekpyrotic-like scenario, one can suppose that the distance between branes increases through the history of the Universe. At the early epoch after the Big Bang, g could be in agreement with the conditions required for the baryogenesis ($g \sim m_Q^2/M_B \sim 10^{-11}$ eV). While the distance increases – for instance up to $d \sim 16m_Q^{-1} \sim 4 \times 10^{-13}$ m – g could drop until current constraints deduced from the photon mass. Nevertheless, the scalar field could offer a dark matter candidate in terms of a field with a non-zero but very weak coupling with the electromagnetic field. This

makes such a scalar field a candidate for optical devices designed for scalar fields detection. Therefore, experiments aiming at constraining such scalar waves play a crucial role to explore braneworld scenarios [83, 84]. In contrast to direct passing-through-wall neutron experiments [38–41], this approach offers a novel method for placing constraints on g . Additionally, one could assume the existence of many effective scalar fields, each one being a partner of a quark of a given type and generation. As explained earlier, ϕ (see Eq. (5)) represents the extra component of the electromagnetic field in the bulk, dressed by the associated quark field, and g is dependent on the constituent mass of the quark (see Eq. (1)). Consequently, a family of scalar fields with distinct masses m_φ could exist. These scalar fields could also be candidates for dark matter [85–89]. Finally, it cannot be excluded that other definitions of the field strength (see Eq. (6)) could be consistent with our baryogenesis scenario while avoiding the problem of the mass of the photon. Nonetheless, exploring those aspects is beyond the scope of the present paper and is left for future investigations.

IX. CONCLUSION

Thanks to the low-energy limit of a two-brane universe – resulting into a noncommutative two-sheeted space-time – it has been demonstrated that the exchange of matter between two branes does not occur at the same rate for antimatter. This discrepancy results from a violation of the C/CP symmetry induced by the scalar field that emerges due to the extension of the electromagnetic gauge field in the two-brane system. This provides a simple physical mechanism allowing baryogenesis to occur lately after the quark-gluon era without strong parameter constraints in cosmological braneworld scenarios. Furthermore, one highlights the importance of any experimental endeavor to constrain scalar waves as dark matter candidates that are able to constrain the present model. Scenarios with definitions of the field strength different from that used in the present paper could be explored in future work, both theoretically and experimentally. Finally, one also intends to provide a comprehensive analysis of the dynamics of additional particles – including other baryons, mesons, and leptons – in the description of baryogenesis.

ACKNOWLEDGMENT

The authors thank Patrick Peter for encouraging us to explore this topic as well as for discussions and comments on an earlier draft of this paper.

[1] A. Arbey, F. Mahmoudi, Dark matter and the early Universe: a review, Prog. Part. Nucl. Phys. **119**, 103865

(2021).

- [2] D. Bodeker, W. Buchmuller, Baryogenesis from the weak scale to the grand unification scale, *Rev. Mod. Phys.* **93**, 035004 (2021).
- [3] J.M. Cline, TASI Lectures on Early Universe Cosmology: Inflation, Baryogenesis and Dark Matter, *PoS TASI2018*, 001 (2019).
- [4] L. Canetti, M. Drewes, M. Shaposhnikov, Matter and Antimatter in the Universe, *New J. Phys.* **14**, 095012 (2012).
- [5] H.M. Lee, Lectures on Physics Beyond the Standard Model, *J. Korean Phys. Soc.* **78**, 985 (2021).
- [6] T.S. Virdee, Beyond the standard model of particle physics, *Phil. Trans.R. Soc. A* **374**, 20150259 (2016).
- [7] Ph. Brax, C. van de Bruck, Cosmology and Brane Worlds: A Review, *Class. Quant. Grav.* **20**, R201 (2003).
- [8] L.B. Okun, Mirror particles and mirror matter: 50 years of speculation and search, *Phys. Usp.* **50**, 380 (2007).
- [9] V.A. Rubakov, M.E. Shaposhnikov, Do we live inside a domain wall?, *Phys. Lett.* **125B**, 136 (1983).
- [10] K. Akama, An Early Proposal of "Brane World", *Lect. Notes Phys.* **176**, 267 (1983).
- [11] M. Pavsic, An Alternative to Matter Localization in the "Brane World": An Early Proposal and its Later Improvements, *Phys. Lett. A* **116**, 1 (1986).
- [12] J. Hughes, J. Liu, J. Polchinski, Supermembranes, *Phys. Lett. B* **180**, 370 (1986).
- [13] P. Horava, E. Witten, Eleven-Dimensional Supergravity on a Manifold with Boundary, *Nucl. Phys.* **B460**, 506 (1996).
- [14] A. Lukas, B.A. Ovrut, K.S. Stelle, D. Waldram, Universe as a domain wall, *Phys. Rev. D* **59**, 086001 (1999).
- [15] R. Davies, D.P. George, R.R. Volkas, Standard model on a domain-wall brane?, *Phys. Rev. D* **77**, 124038 (2008).
- [16] R. Maartens, K. Koyama, Brane-World Gravity, *Living Rev. Relativity* **13**, 5 (2010).
- [17] P. Brax, C. van de Bruck, A.-C. Davis, Brane world cosmology, *Rep. Prog. Phys.* **67**, 2183 (2004).
- [18] T. Koivisto, D. Wills and I. Zavala, Dark D-brane cosmology, *JCAP* **06**, 036 (2014).
- [19] N. Arkani-Hamed, S. Dimopoulos, N. Kaloper and G. Dvali, Manyfold universe, *JHEP* **12**, 010 (2000).
- [20] S. Bhattacharya, S.R. Kousvos, S. Romanopoulos, T.N. Tomaras, Cosmological screening and the phantom braneworld model, *Eur. Phys. J. C* **78**, 637 (2018).
- [21] S. Bhattacharya, S.R. Kousvos, Constraining phantom braneworld model from cosmic structure sizes, *Phys. Rev. D* **96**, 104006 (2017).
- [22] D. Battefeld, P. Peter, A Critical Review of Classical Bouncing Cosmologies, *Phys. Rept.* **571**, 1 (2015).
- [23] J. Omotani, P.M. Saffin, J. Louko, Colliding branes and big crunches, *Phys. Rev. D* **84**, 063526 (2011).
- [24] G. Gibbons, K. i. Maeda and Y. i. Takamizu, Fermions on Colliding Branes, *Phys. Lett. B* **647**, 1 (2007).
- [25] P.M. Saffin, A. Tranberg, Particle transfer in braneworld collisions, *JHEP* **0708**, 072 (2007).
- [26] P.M. Saffin, A. Tranberg, The fermion spectrum in braneworld collisions, *JHEP* **0712**, 053 (2007).
- [27] G.W. Gibbons, H. Lu, C.N. Pope, Brane Worlds in Collision, *Phys. Rev. Lett.* **94**, 131602 (2005).
- [28] J. Ponce de Leon, Brane-world models emerging from collisions of plane waves in 5D, *Gen. Rel. Grav.* **36**, 923 (2004).
- [29] Y.I. Takamizu, K.I. Maeda, Collision of Domain Walls and Reheating of the Brane Universe, *Phys. Rev. D* **70**, 123514 (2004).
- [30] U. Gen, A. Ishibashi, T. Tanaka, Brane Big-Bang Brought by Bulk Bubble, *Phys. Rev. D* **66**, 023519 (2002).
- [31] D. Langlois, K.I. Maeda, D. Wands, Conservation Laws for Collisions of Branes and Shells in General Relativity, *Phys. Rev. Lett.* **88**, 181301 (2002).
- [32] M. Bastero-Gil, E.J. Copeland, J. Gray, A. Lukas, M. Plumacher, Baryogenesis by Brane-Collision, *Phys. Rev. D* **66**, 066005 (2002).
- [33] J. Khoury, B.A. Ovrut, P.J. Steinhardt, N. Turok, Ekpyrotic universe: Colliding branes and the origin of the hot big bang, *Phys. Rev. D* **64**, 123522 (2001).
- [34] G. Dvali, G. Gabadadze, Non-conservation of Global Charges in the Brane Universe and Baryogenesis, *Phys. Lett.* **B460**, 47 (1999).
- [35] Z. Berezhiani, Unified picture of ordinary and dark matter genesis, *Eur. Phys. J. Special Topics* **163**, 271 (2008).
- [36] M. Sarrazin, F. Petit, Brane matter, hidden or mirror matter, their various avatars and mixings: many faces of the same physics, *Eur. Phys. J. C* **72** (2012) 2230.
- [37] M. Sarrazin, G. Pignol, F. Petit, V. V. Nesvizhevsky, Experimental limits on neutron disappearance into another braneworld, *Phys. Lett. B* **712**, 213 (2012).
- [38] M. Sarrazin, G. Pignol, J. Lamblin, F. Petit, G. Terwagne, V.V. Nesvizhevsky, Probing the braneworld hypothesis with a neutron-shining-through-a-wall experiment, *Phys. Rev. D* **91**, 075013 (2015).
- [39] M. Sarrazin, G. Pignol, J. Lamblin, J. Pinon, O. Meplan, G. Terwagne, P.-L. Debarsy, F. Petit, V.V. Nesvizhevsky, Search for passing-through-walls neutrons constrains hidden braneworlds, *Phys. Lett. B* **758**, 14 (2016).
- [40] C. Stasser, G. Terwagne, J. Lamblin, O. Méplan, G. Pignol, B. Coupé, S. Kalcheva, S. Van Dyck, M. Sarrazin, Probing neutron-hidden neutron transitions with the MURMUR experiment, *Eur. Phys. J. C* **81**, 17 (2021).
- [41] H. Almazán, L. Bernard, A. Blanchet, A. Bonhomme, C. Buck, P. del Amo Sanchez, *et al.*, Searching for Hidden Neutrons with a Reactor Neutrino Experiment: Constraints from the STEREO Experiment, *Phys. Rev. Lett.* **128**, 061801 (2022).
- [42] L.J. Broussard, J.L. Barrow, L. DeBeer-Schmitt, T. Dennis, M.R. Fitzsimmons, M.J. Frost, *et al.*, Experimental Search for Neutron to Mirror Neutron Oscillations as an Explanation of the Neutron Lifetime Anomaly, *Phys. Rev. Lett.* **128**, 212503 (2022).
- [43] M. Hostert, D. McKeen, M. Pospelov, N. Raj, Dark sectors in neutron-shining-through-a-wall and nuclear absorption signals, *Phys. Rev. D* **107**, 075034 (2023).
- [44] F. Petit, M. Sarrazin, Quantum dynamics of massive particles in a non-commutative two-sheeted space-time, *Phys. Lett. B* **612**, 105 (2005).
- [45] M. Sarrazin, F. Petit, Equivalence between domain-walls and "noncommutative" two-sheeted spacetimes: Model-independent matter swapping between branes, *Phys. Rev. D* **81**, 035014 (2010).
- [46] C. Stasser, M. Sarrazin, Sub-GeV-scale signatures of hidden braneworlds up to the Planck scale in a $SO(3,1)$ -broken bulk, *Int. J. Mod. Phys. A* **34**, 1950029 (2019).
- [47] C. Stasser, M. Sarrazin, Can neutron disappearance/reappearance experiments definitively rule out the existence of hidden braneworlds endowed with a copy of the Standard Model?, *Int. J. Mod. Phys. A* **35**, 2050202

- (2020).
- [48] A. Sakharov, Violation of CP Invariance, C Asymmetry, and Baryon Asymmetry of the Universe, JETP Letters **5**, 24 (1967).
 - [49] M. Sarrazin, F. Petit, Exciton swapping in a twisted graphene bilayer as a solid-state realization of a two-brane model, Eur. Phys. J. B **87**, 26 (2014).
 - [50] D. Griffiths, *Introduction to Elementary Particles*, Wiley-VCH Verlag GmbH & Co. KGaA (2008).
 - [51] W. Lucha, F.F. Schöberl, D. Gromes, Bound states of quarks, Phys. Rep. **200**, 127 (1991).
 - [52] H.J. Lipkin, The constituent quark model revisited. Masses and magnetic moments, Phys. Lett. B **233**, 446 (1989).
 - [53] I. Cohen, H.J. Lipkin, Why masses and magnetic moments satisfy naive quark model predictions, Phys. Lett. **93B**, 56 (1980).
 - [54] A. Connes, J. Lott, Particle Models and Concommutative Geometry, Nucl. Phys. B **18** (Proc.Suppl.), 29 (1990).
 - [55] F. Lizzi, G. Mangano, G. Miele, G. Sparano, Fermion Hilbert Space and Fermion Doubling in the Noncommutative Geometry Approach to Gauge Theories, Phys. Rev. D **55**, 6357 (1997).
 - [56] F. Lizzi, G. Mangano, G. Miele, G. Sparano, Mirror Fermions in Noncommutative Geometry, Mod. Phys. Lett. A **13**, 231 (1998).
 - [57] J.M. Gracia-Bondia, B. Iochum, T. Schucker, The standard model in noncommutative geometry and fermion doubling, Phys. Lett. B **416**, 123 (1998).
 - [58] H. Kase, K. Morita, Y. Okumura, Lagrangian Formulation of Connes' Gauge Theory, Prog. Theor. Phys. **101**, 1093 (1999).
 - [59] H. Kase, K. Morita, Y. Okumura, A Field-Theoretic Approach to Connes' Gauge Theory on $M_4 \times Z_2$, Int. J. Mod. Phys. A **16**, 3203 (2001).
 - [60] C. Macesanu, K. C. Wali, The Higgs Sector on a Two-Sheeted Space Time, Int. J. Mod. Phys. A **21**, 4519 (2006).
 - [61] Ch. Brouder, N. Bizi, F. Besnard, The Standard Model as an extension of the noncommutative algebra of forms, hal-01142491 (2015).
 - [62] P.T. Chrusciel, On Space-Times with $U(1) \otimes U(1)$ Symmetric Compact Cauchy Surfaces, Ann. Phys. **202**, 100 (1990).
 - [63] P. Forgács, Á. Lukács, Stabilisation of semilocal strings by dark scalar condensates, Phys. Rev. D **95**, 035003 (2017).
 - [64] M. Sarrazin, F. Petit, Matter localization and resonant deconfinement in a two-sheeted spacetime, Int. J. Mod. Phys. A **22**, 2629 (2007).
 - [65] M. Kachelriess, *Quantum Fields from the Hubble to the Planck Scale*, Oxford Graduate Texts (2018).
 - [66] P. Peter, J.-P. Uzan, *Primordial Cosmology*, Oxford Graduate Texts (2013).
 - [67] B.W. Lee, S. Weinberg, Cosmological Lower Bound on Heavy-Neutrino Masses, Phys. Rev. Lett. **39**, 165 (1977).
 - [68] A. Riotto, Inflation and the theory of cosmological perturbations, ICTP Ser. Theor. Phys. **15** (1999).
 - [69] D. Manzano, A short introduction to the Lindblad master equation, AIP Advances **10**, 025106 (2020).
 - [70] M. Cannoni, Relativistic $\langle \sigma v_{rel} \rangle$ in the calculation of relics abundances: A closer look, Phys. Rev. D **89**, 103533 (2014).
 - [71] D. Grasso, H.R. Rubinstein, Magnetic Fields in the Early Universe, Phys. Rept. **348**, 163 (2001).
 - [72] B. Cheng and A. Olinto, Primordial magnetic fields generated in the quark-hadron transition, Phys. Rev. D **50**, 2421 (1994).
 - [73] L. Husdal, On Effective Degrees of Freedom in the Early Universe, Galaxies, **4**, 78 (2016).
 - [74] D.V. Bugg, J. Hall, A.S. Clough, R.L. Shypit, K. Bos, J.C. Kluyver, *et al.*, $\bar{p}p$ total cross sections below 420 MeV/c, Phys. Lett. B **194**, 563 (1987).
 - [75] OBELIX Collaboration, Antineutron-proton total cross section from 50 to 400 MeV/c, Phys. Lett. B **475**, 378 (2000).
 - [76] A. Zenoni, A. Bianconi, F. Bocci, G. Bonomi, M. Corradini, A. Donzella, *et al.*, New measurements of the $\bar{p}p$ annihilation cross section at very low energy, Phys. Lett. B **461**, 405 (1999).
 - [77] G.F. Chew, Forces between nucleons and antinucleons, PNAS **45**, 456 (1959).
 - [78] M. Astrua, E. Botta, T. Bressani, D. Calvo, C. Casalegno, A. Feliciello, A. Filippi, S. Marcello, M. Agnello, F. Iazzi, Antineutron-nucleus annihilation cross sections below 400 MeV/c, Nucl. Phys. A **697**, 209 (2002).
 - [79] F. Englert, R. Brout, Broken Symmetry and the Mass of Gauge Vector Mesons, Phys. Rev. Lett. **13**, 321 (1964).
 - [80] P.W. Higgs, Broken Symmetries and the Masses of Gauge Bosons, Phys. Rev. Lett. **13**, 508 (1964).
 - [81] G.S. Guralnik, C.R. Hagen, and T.W.B. Kibble, Global Conservation Laws and Massless Particles, Phys. Rev. Lett. **13**, 585 (1964).
 - [82] R.L. Workman, V.D. Burkert, V. Crede, E. Klempt, U. Thoma, L. Tiator, *et al.* (Particle Data Group), Review of Particle Physics, Prog. Theor. Exp. Phys. **2022**, 083C01 (2022).
 - [83] A. Hees, O. Minazzoli, E. Savalle, Y. V. Stadnik, P. Wolf, Violation of the equivalence principle from light scalar dark matter, Phys. Rev. D **98**, 064051 (2018).
 - [84] E. Savalle, A. Hees, F. Frank, E. Cantin, P.-E. Pottie, B. M. Roberts, L. Cros, B.T. McAllister, P. Wolf, Searching for dark matter with an unequal delay interferometer, Phys. Rev. Lett. **126**, 051301 (2021).
 - [85] A.X. González-Morales, D.J.E. Marsh, J. Peñarrubia, L.A. Ureña-López, Unbiased constraints on ultralight axion mass from dwarf spheroidal galaxies, MNRAS **472**, 1346 (2017).
 - [86] M. Buschmann, R.T. Co, C. Dessert, B.R. Safdi, Axion Emission Can Explain a New Hard X-Ray Excess from Nearby Isolated Neutron Stars, Phys. Rev. Lett. **126**, 021102 (2021).
 - [87] J. Solís-López, F.S. Guzmán, T. Matos, V.H. Robles, L.A. Ureña-López, Scalar field dark matter as an alternative explanation for the anisotropic distribution of satellite galaxies, Phys. Rev. D **103**, 083535 (2021).
 - [88] E.O. Nadler, A. Drlica-Wagner, K. Bechtol, S. Mau, R.H. Wechsler, V. Gluscevic, *et al.* (DES Collaboration), Constraints on Dark Matter Properties from Observations of Milky Way Satellite Galaxies, Phys. Rev. Lett. **126**, 091101 (2021).
 - [89] A. Amruth *et al.*, Einstein rings modulated by wavelike dark matter from anomalies in gravitationally lensed images, Nat. Astron. **7**, 736 (2023).